

**ISTANBUL TECHNICAL UNIVERSITY ★ ENERGY INSTITUTE**

**CHARACTERIZATION OF ELECTROCHEMICALLY  
PREPARED CIS THIN FILMS**

**M.Sc. THESIS**

**Gizem ŞANLI**

**Department of Energy Science and Technology**

**Energy Science and Technology Programme**

**MARCH 2013**



**ISTANBUL TECHNICAL UNIVERSITY ★ ENERGY INSTITUTE**

**CHARACTERIZATION OF ELECTROCHEMICALLY  
PREPARED CIS THIN FILMS**

**M.Sc. THESIS**

**Gizem ŞANLI  
(301081043)**

**Department of Energy Science and Technology  
Energy Science and Technology Programme**

**Thesis Advisor: Prof. Dr. Figen KADIRGAN**

**MARCH 2013**



**İSTANBUL TEKNİK ÜNİVERSİTESİ ★ ENERJİ ENSTİTÜSÜ**

**CHARACTERIZATION OF ELECTROCHEMICALLY  
PREPARED CIS THIN FILMS  
ELEKTROKİMYASAL YÖNTEMLERLE HAZIRLANMIŞ CIS İNCE  
FİLMLERİNİN KARAKTERİZASYONU**

**YÜKSEK LİSANS TEZİ**

**Gizem ŞANLI  
(301081043)**

**Enerji Bilim ve Teknoloji Anabilim Dalı**

**Enerji Bilim ve Teknoloji Programı**

**Tez Danışmanı: Prof. Dr. Figen KADIRGAN**

**MART 2013**



Gizem Şanlı, a M.Sc. student of ITU Energy Institute, student ID 301081043, successfully defended the thesis entitled "Characterization of Electrochemically Prepared CIS Thin Films", which she prepared after fulfilling the requirements specified in the associated legislations, before the jury whose signatures are below.

**Thesis Advisor :**      **Prof. Dr. Figen KADIRGAN**  
İstanbul Technical University

**Jury Members :**      **Prof. Dr. Nilgün Yavuz (İTÜ)**  
**Prof. Dr. Birsen Demirata Öztürk (İTÜ)**

**Date of Submission : 17 December 2012**

**Date of Defense : 23 January 2013**





## TABLE OF CONTENTS

	Page
<b>TABLE OF CONTENTS</b> .....	vii
<b>LIST OF TABLES</b> .....	ix
<b>LIST OF FIGURES</b> .....	x
<b>SUMMARY</b> .....	xi
<b>ÖZET</b> .....	xii
<b>1. INTRODUCTION</b> .....	1
1.1 Experimental techniques .....	2
1.1.1 Cyclic voltammetry.....	2
1.1.2 Potentiostatic coulometry .....	2
1.1.3 Ultraviolet-visible spectroscopy.....	3
1.1.4 X-ray diffraction .....	4
1.1.5 Scanning electron microscopy .....	4
1.1.6 Energy dispersive spectroscopy.....	5
<b>2. PHOTOVOLTAICS</b> .....	7
2.1 History.....	7
2.2 Physics of Solar Cells .....	7
2.3 Thin Film Solar Cells .....	8
<b>3. Cu(In,Ga)Se<sub>2</sub> THIN FILMS</b> .....	11
3.1 Structural Properties.....	11
3.2 Electrical properties .....	12
3.3 Optical properties .....	12
<b>4. Cu(In,Ga)Se<sub>2</sub> THIN FILM DEPOSITION METHODS</b> .....	15

4.1 Co-evaporation .....	15
4.2 Sputtering .....	16
4.3 Chemical vapor deposition .....	16
4.4 Co-electrodeposition .....	17
<b>5. EXPERIMENTAL DETAILS .....</b>	<b>19</b>
5.1 Experimental Setup.....	19
5.2 Sample Preparation .....	20
<b>6. RESULTS AND CONCLUSION.....</b>	<b>21</b>
6.1 Spectroscopy Results .....	21
6.2 XRD Results .....	26
6.3 EDS Results.....	28
6.4 SEM Results.....	30
6.5 Conclusion.....	32
<b>7. REFERENCES.....</b>	<b>33</b>

## LIST OF TABLES

	<u>Page</u>
<b>Table 6.1:</b> Cu(In,Ga)Se <sub>2</sub> solar cell structure.....	25
<b>Table 6.2:</b> Charge carrier generation.....	25
<b>Table 6.3:</b> Atomic Structure of Cu(In,Ga)Se <sub>2</sub> .....	26

## LIST OF FIGURES

	<u>Page</u>
<b>Figure 2.1:</b> Cu(In,Ga)Se <sub>2</sub> solar cell structure.....	6
<b>Figure 2.2:</b> Charge carrier generation.....	7
<b>Figure 3.1:</b> Atomic Structure of Cu(In,Ga)Se <sub>2</sub> .....	9
<b>Figure 3.2:</b> EG vs Ga.....	10
<b>Figure 3.3:</b> Absorption coefficient of CuIn <sub>x</sub> Ga <sub>1-x</sub> Se <sub>2</sub> (x=1, 0.8, 0.6, 0.4, 0.2 and 0).....	11
<b>Figure 5.1:</b> The three-electrode setup used in electrodeposition.....	16
<b>Figure 6.1:</b> Optical absorbance ( $\alpha$ ) vs. wavelength (nm).....	18
<b>Figure 6.2:</b> Optical absorbance ( $\alpha$ ) vs. wavelength (nm).....	19
<b>Figure 6.3:</b> Optical absorbance ( $\alpha$ ) vs. wavelength (nm).....	19
<b>Figure 6.4:</b> Optical absorbance ( $\alpha$ ) vs. wavelength (nm).....	20
<b>Figure 6.5:</b> Optical absorbance ( $\alpha$ ) vs. wavelength (nm) after annealing.....	21
<b>Figure 6.6:</b> ( $\alpha h\nu$ ) <sup>2</sup> vs. $h\nu$ .....	22
<b>Figure 6.7:</b> XRD patterns of CIS films.....	23
<b>Figure 6.8:</b> XRD patterns of CIS films.....	23
<b>Figure 6.9:</b> XRD patterns of CIS films annealed at 400 <sup>0</sup> C for 30 min. ....	24
<b>Figure 6.10:</b> SEM image of sample 1a.....	27
<b>Figure 6.11:</b> SEM image of sample 2a.....	27
<b>Figure 6.12:</b> SEM image of sample 3a.....	28

## **CHARACTERIZATION OF ELECTROCHEMICALLY PREPARED CIS THIN FILMS**

### **SUMMARY**

As the energy demand in the world increases, more and more extensive research is undertaken concerning renewable energy sources. Developing reliable and low-cost technologies to make use of renewable energy sources is the main objective of many research topics. Several researches are on-going to develop efficient photovoltaic devices which are used to convert solar energy directly to electricity.

New generation thin film solar cells are rapidly replacing the traditional Si solar cells because less material is needed and they can be produced at a lower cost. Among the thin film solar cell materials, CIS has attracted research due to its high potential, having a direct band-gap within the maximum solar absorption region, a high absorption coefficient and appropriate electrical and optical properties for production, as has been demonstrated by the ~20% conversion efficiency.

The working mechanism of the CIS devices is not well understood and the causes of defects in the electrical structure are not well known. Structural defects, principles of the solid-state physics, manufacturing methods, functioning of the device and efficiency losses found in laboratory conditions should be studied in order to design and manufacture high efficiency solar cells. The subject of this study is to investigate and evaluate the CIS solar cells prepared by electro-deposition and to determine the conditions at which the cells work more efficiently.

The electro-deposition was carried out in an electrochemical cell using a standard three-electrode system. The reference electrode was saturated calomel electrode, the counter electrode was Pt gauze, and the working electrode was a ITO-coated soda lime glass substrate. Films were deposited in an unstirred bath for 15 minutes at room temperature, at -650mV as determined by cyclic voltammograms. The deposited films were rinsed with distilled water, dried in N<sub>2</sub> gas, and selenized with Ar at 400°C. The structural and optical properties of the films were analyzed by UV-spectroscopy, X-Ray Diffraction and scanning electron microscopy.

## ELEKTROKİMYASAL YÖNTEMLERLE HAZIRLANMIŞ CIS İNCE FİMLERİNİN KARAKTERİZASYONU

### ÖZET

Önümüzdeki 20 yıl içerisinde dünyadaki enerji talebinin önemli ölçüde yükselmesi beklenmektedir. Bu yükseliş nedeniyle de alternatif enerji kaynaklarına olan ilgi artmıştır.

Günümüzde elektrik üretiminin büyük bir kısmı fosil yakıtlarla karşılanmaktadır. Kaynakların hızla tükenmesi ve yakıtların elektrik enerjisine dönüştürülürken ürettikleri zararlı gazlar nedeniyle çevreyi kirletmesi yenilenebilir, temiz enerji kaynaklarına gösterilen ilgi ve verilen önemin artmasına sebep olmuştur.

Önemli çevre dostu enerji kaynaklarından biri güneştir. Güneş enerjisini doğrudan elektrik enerjisine çevirebilmek için güneş hücreleri kullanılmaktadır. Bunlar geleneksel ve yeni nesil olmak üzere iki çeşittir.

Geleneksel güneş hücreleri kristalik silikondan yapılmaktadır. Ancak, verimlerinin daha yüksek olmasına rağmen, belirli yarı-iletkenlerin üretim için gereken miktarının daha az olması ve daha ucuza üretilebilmeleri nedeniyle yerini yeni nesil polikristalik ince-film güneş hücrelerine bırakmaktadır.

İnce-film güneş hücrelerinin 3 temel çeşidi bulunmaktadır. Bunlar kullanılan yarı-iletkenlere göre farklılık gösteren amorf-silisyum (a-Si), kadmiyum tellürid (CdTe) ve bakır indiyum (galyum) di-selenid'dir (CI(G)S).

CIGS, tetragonal yapıda bir yarı-iletkenidir. İnce film güneş hücrelerinde ışık emici malzeme olarak kullanılmaktadır. Direkt geçişli bant yapısı, uygun bant aralığı(1.05eV-1.68eV), yüksek soğurma katsayısı ( $\sim 10^5 \text{ Cm}^{-1}$ ), uygun elektriksel ve optiksel yapısı ve çeşitli üretim yöntemleri için uygun olması nedeniyle yüksek verim elde edilebilen CIGS'ler fotovoltaik alanın önemli bir araştırma konusudur.

Polikristal CIS ince filmlerin üretilmesinde piroliz, püskürtme, buharlaştırma, epitaksi, selenleştirme gibi yöntemler kullanılmaktadır. Elektrokaplama yöntemi ise ucuz olması, vakum işlemler gerektirmemesi ve zehirli gazlar kullanılmaması sebebiyle tercih edilen bir yöntemdir. Sadece 1-2  $\mu\text{m}$  kalınlığında olan CIS'ler bu yöntemle cam veya folyo üzerine monte edilebilirler. Günümüzde genellikle cam kullanılan düzenlere rastlanmaktadır. Elektrokaplama ile hazırlanan CIS güneş pillerinin yüzey morfolojisi, element bileşimi, kristal yapısı, optoelektronik özellikleri ve kuantum verimliliği çeşitli makalelerde incelenmiştir.

CI(G)S'ler p-tipi veya n-tipi olabilirler. Yüksek kaliteli fotovoltaik sistemlerde kullanılan CI(G)S filmler selenyum zengin ortamda üretilen p-tipi yarı-iletkenlerdir.

Laboratuvar ortamında kaydedilmiş olan en yüksek verim  $\sim 19,5\%$ 'tur. Bu yüksek verim CIGS'in yüksek soğurma katsayısı, direkt geçişli bant yapısı, uygun yasak enerji bant aralığı ve uygun elektriksel ve optiksel yapısı sayesinde elde edilmiştir. CI(G)S'in yüksek soğurma katsayısı filmde güneş ışın şiddetinin  $\%95$ 'inin soğurulması imkan sağlamaktadır.

CI(G)S kullanılan sistemlerde cihazların davranış biçimleri tam olarak anlaşılmamaktadır. Elektriksel yapı bozukluklarının kaynakları tam olarak bilinmemektedir. Yapısal bozuklukları, katı-hal fiziği prensiplerini, üretim aşamalarını, cihazın nasıl çalıştığını ve laboratuvar ortamında elde edilen değerlerdeki verimlilik kayıplarının sebebini anlamak daha yüksek verimli sistemler tasarlayabilmek ve üretebilmek için gereklidir.

Filmlerin kristalik yapısı, kompozisyonu, yüzey morfolojisi, yasak bant genişliği ve elektriksel özellikleri güneş hücrelerinin verimli çalışmasıyla doğrudan ilgili olduğu için, nasıl çalıştıklarının incelenmesi gerekmektedir.

Elektrokimyasal yöntemle kaplanan CIS filmler UV-spektroskopi, X-Ray kırınımı, tarama elektron mikroskobu ve enerji dağılım spektroskopi yöntemleri ile incelenmiştir.





## 1. INTRODUCTION

Along with the growth in industrialization and the expanding population, the energy demand in world is expected to increase rapidly in the following decades [1]. Today, most of the electricity is generated by fossil fuels. Rapid consumption of the limited sources and the increase in environmental pollution has drawn more attention to clean and renewable energy sources.

Due to the need for low-cost, clean and renewable energy sources, direct conversion of solar energy to electrical energy by solar cells is an important research topic at present. Solar cells are easy to install and use, and they have long operational lifetimes, which eliminates the need for continuous maintenance. Due to its reliability and stability, solar energy combined with short-term storage devices is a good choice for electricity production [2].

There are two types of solar cells; traditional Si and new generation thin film. Although their higher conversion efficiencies, traditional Si solar cells are being rapidly replaced by the new generation solar cells because less material is needed and they can be produced at a lower cost. Among the thin film solar cell materials, Cu(In,Ga)Se has attracted special attention in research due to its high potential, having a direct band-gap within the maximum solar absorption region, a high absorption coefficient and appropriate electrical and optical properties for production, as has been demonstrated by the ~20% conversion efficiency [3].

There is a wide variety of technologies for CIS-based thin film production; such as physical evaporation and sputtering techniques, as well as chemical methods. Although highest efficiencies have been achieved by the first two high-vacuum techniques, they are undesirable with their expensive thermal/cryogenic requirements and complexity of processes [4]. On the other hand, electrochemical methods are suitable with scientific, technological and economic benefits. The simplest electrochemical method is electrodeposition and it deserves special attention because it has shown to be a non-vacuum, inexpensive, non-polluting, easily scalable method

having a high deposition speed [4-6]. Efficiencies up to 15.4% have been obtained by the electrodeposition technique [7].

The working mechanism of the CIS-based thin film devices is not well understood and the causes of defects in the electrical structure are not well known. Structural defects, principles of the solid-state physics, manufacturing methods, functioning of the device and efficiency losses found in laboratory conditions should be studied in order to design and manufacture high efficiency solar cells. The subject of this study is to investigate and evaluate the electrical and optical properties of CIS-based solar cells prepared by electrodeposition and to determine the conditions at which the cells work more efficiently.

## **1.1 Experimental techniques**

### **1.1.1 Cyclic voltammetry**

Cyclic voltammetry is an electrochemical technique used to study the process taking place at the electrode-electrolyte interface. The potential range is scanned in a cycle, starting at the initial potential, being inverted at the final potential, and ending at the initial potential. The potential is applied between the reference electrode and the working electrode and the current between the working electrode and the counter electrode is measured. The collected data is plotted as current vs. potential. During the potential scan, when the potential reaches the reduction potential of the compound in the electrolyte, the compound is reduced and the current increases; but then falls off as the concentration of ions at the electrode surface decreases. As a result, the reduction potential of a particular material to be deposited can be determined. [6]

The reduction potentials of the materials used in the experiments were determined by cyclic voltammetry measurements using Volta-Lab PGZ 301.

### **1.1.2 Potentiostatic coulometry**

Coulometry is an analytical method capable of measuring the quantity of matter transformed during an electrolysis reaction by measuring the amount of current flowing through the circuit.

In principle, as long as the cell volume is accurately known and the electrolysis is carried out to completion, the corresponding charge is an absolute determinant of the analyte quantity and concentration [24].

In potentiostatic coulometry, electric potential of the working electrode is kept constant during the reaction by using a potentiostat. The mass transfer of the compounds in the solution to the electrode surface is measured as the current flowing through the circuit, in Coulombs.

In the experiments, potentiostatic coulometry measurements were done at -650mV using Volta-Lab PGZ 301.

### 1.1.3 Ultraviolet-visible spectroscopy

In UV-Vis Spectroscopy, light in the visible and near-ultraviolet region is used and the optical properties such as absorbance, transmittance and reflectance are measured as a function of wavelength. The working principle of the spectrophotometer is as follows:

In a double beam spectrophotometer, light is split into two beams. One beam passes through the reference (undeposited) cell and the other beam passes through to the sample (deposited cell). The intensities of the two beams are measured and the ratio of the two beams is calculated either as absorbance (%A) or transmittance (%T).

$$A = \ln(I_0/I) = -\ln T \quad (1.1)$$

where  $I_0$  is the intensity of light passing through the reference cell, and  $I$  is the intensity of light passing through the sample.

The obtained optical measurement values are used to calculate the absorption coefficient of the sample using the following formula:

$$\alpha = \frac{\ln[T/(1-R)^2]}{d} \quad (1.2)$$

where  $T$  is optical transmittance (%),  $R$  is reflectance (%) and  $d$  is the thickness of the film (cm) [3].

Also, the band gap of the sample is calculated using the following equation:

$$\alpha = \frac{A}{h\nu} \sqrt{(h\nu - E_g)} \quad (1.3)$$

where  $A$  is a constant, depending on the refractive index of the material,  $h\nu$  is the radiation energy, and  $E_g$  is the transition energy [20].

The optical absorbance of the electrodeposited CIS layer was measured by T80+ UV/VIS Spectrophotometer.

#### **1.1.4 X-ray diffraction**

X-ray diffraction (XRD) is a powerful technique used to identify the crystalline structures of materials and to measure the structural properties of the phases in the structure.

The samples are irradiated with collimated x-rays and scattered according to the samples' crystal structure. XRD is constructive interference of the scattered waves. From the diffraction pattern, the size and symmetry of the crystal structure can be calculated.

Polycrystalline thin films can have a distribution of orientations, which influences the thin-film properties. And, XRD is an ideal method to use since it is a noncontact and nondestructive technique.

The most important use of thin-film XRD is phase identification. For films possessing several phases, the proportion of each phase can be determined from the integrated intensities in the diffraction pattern.

Characterization measurements, using the XRD Philips PW 3710, were done at the Chemical & Metallurgical Engineering Faculty of ITU.

#### **1.1.5 Scanning electron microscopy**

Scanning electron microscopy (SEM) is a useful technique used to analyze the surface morphology of a sample from hundreds of  $\mu\text{m}$  to sub  $\mu\text{m}$  scale. Grain sizes and shapes of absorber films can be determined by SEM.

Image analysis is done by focusing a source electron beam into a probe and scanning over the surface of the sample. Secondary electron and backscattered images are obtained and they provide the topographical information of the surface.

SEM characterization measurements were done, using JOEL JCM 7000F, at the Chemical & Metallurgical Engineering Faculty of ITU.

### **1.1.6 Energy dispersive spectroscopy**

Energy dispersive spectroscopy (EDS) is an analytical technique used for elemental analysis or chemical characterization of a sample. It allows the identification of particular elements and their relative proportions.

An EDS system attached to the SEM utilizes the characteristic x-rays emitted from the sample when it is irradiated by the electron beam. Since the characteristics x-rays have unique energies according to the shell of each atom, EDS can be used for both qualitative and quantitative analysis of the sample.

EDS measurements were done, using JOEL JCM 7000F, at the Chemical & Metallurgical Engineering Faculty of ITU.



## 2. PHOTOVOLTAICS

### 2.1 History

The photovoltaic effect, which is creation of electric current in a material upon exposure to light, was first observed in 1839 by Alexandre-Edmond Becquerel while experimenting with an electrolytic cell made up of two metal electrodes. However, it was not until 1883 when the first photovoltaic cell was built, by Charles Fritts. Fritts coated the semiconductor selenium with an extremely thin layer of gold to form the junctions of the device which had less than 1% efficiency.

Solar cells became a more interesting research topic after 1941, when Russell Ohl developed the first silicon p-n junction cell. In 1954, at Bell Laboratories, D. Chapin, C. Fuller and G. Pearson fabricated modern photovoltaic cells with 6% efficiency [8]. In 18 months, they accomplished to develop cells with 10% efficiency [9].

### 2.2 Physics of Solar Cells

A solar cell is a photovoltaic device which converts sunlight directly into electricity. It is basically a p-n heterojunction diode as a result of the contact between the absorber layer and the buffer layer of the cell. These layers are fabricated from a variety of semiconductors and the working mechanism of the device can be understood by applying the basic principles of semiconductor physics.

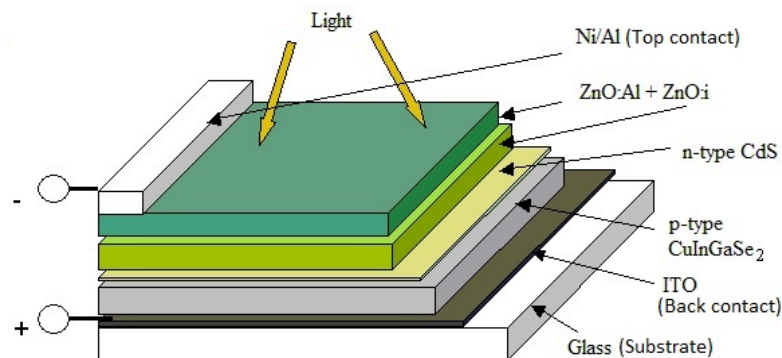


**Figure 2.1:** Cu(In,Ga)Se<sub>2</sub> solar cell structure.

Figure 2.1 shows the schematic structure of Cu(In,Ga)Se<sub>2</sub> solar cells.

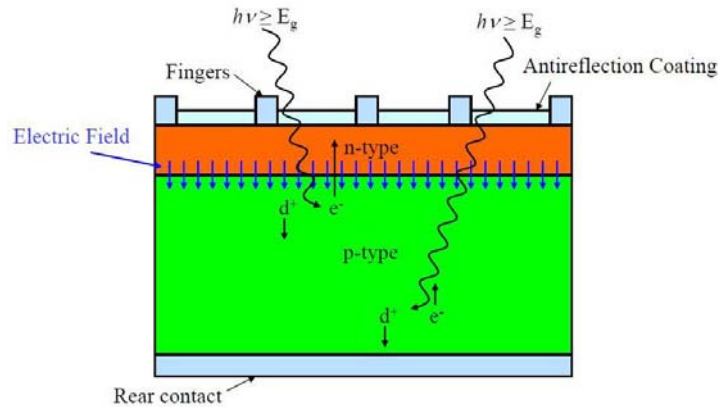


**Figure 2.2:** Charge carrier generation.

When the solar cell is exposed to solar radiation, the absorber layer in the solar cell (CIS) absorbs the sunlight and photons having energies greater than the band gap energy of the semiconductor are converted into electron-hole pairs across the junction (depletion region). These electron-hole pairs, which are also called charge carriers, are separated by the internal electric field of the junction, creating direct current[2]. The charge carrier generation is shown in Figure 2.2.

### 2.3 Thin Film Solar Cells

Highest efficiencies in the photovoltaic industry are achieved by crystalline silicon solar cells. They are readily available as raw material, non-toxic, reliable, and they are fabricated with a mature processing technology [10]. But they have complex manufacturing processes and high production costs. Currently, thin film technologies are being widely investigated by many researchers to decrease the production costs of solar cells by reducing the amount of material used and by applying low-cost manufacturing methods [11]. Another reason they are advantageous is that they can be made into flexible and light-weight modules on alternative substrates [12].

When the available photovoltaic materials are examined, it is seen that the most promising and common thin film materials are amorphous silicon (a-Si) or



polycrystalline materials such as CdTe, CIS and CIGS due to their appropriate band-gap values and high absorption coefficients as well as being able to be grown on a wide variety of substrate materials [13].

One major difference to note between the traditional crystalline silicon and the polycrystalline thin-film devices, beyond the required thickness for sufficient absorption, is the junction type. Silicon devices are composed of p-n homojunctions, whereas polycrystalline films are made from p-n heterojunctions formed between the active absorber material and a window layer [12].



### 3. Cu(In,Ga)Se<sub>2</sub> THIN FILMS

#### 3.1 Structural Properties

Cu(In,Ga)Se<sub>2</sub> belongs among the I-III-VI group of compounds. Both CuInSe<sub>2</sub> and CuGaSe<sub>2</sub> are semiconductor alloys with chalcopyrite lattice structures. They can be mixed in any proportion to form Cu(In,Ga)Se<sub>2</sub> films are very tolerant of variations of composition. When combined into the alloy, the In and Ga occupy the same sites in the lattice and their ratio in crystal is determined by the concentration of the alloy.

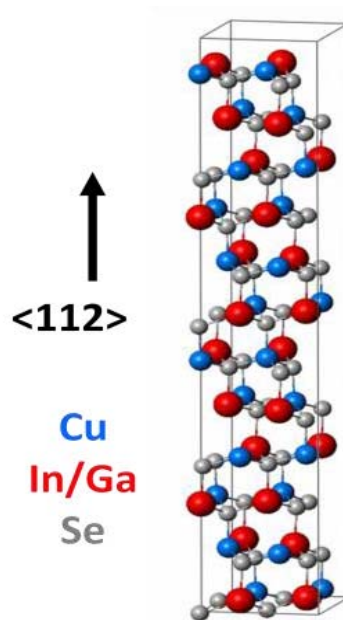


**Figure 3.1:** Atomic Structure of Cu(In,Ga)Se<sub>2</sub>.

The lattice structure of Cu(In,Ga)Se<sub>2</sub> is shown in Figure 3.1. The blue spheres represent Cu, the red spheres either In or Ga depending on the alloy composition and the gray spheres show Se.

The inclusion of gallium in Cu(In,Ga)Se<sub>2</sub> absorber layer has the effect of tuning the bandgap from 1.0 eV for CuInSe<sub>2</sub> to 1.7eV for CuGaS<sub>2</sub> [4].

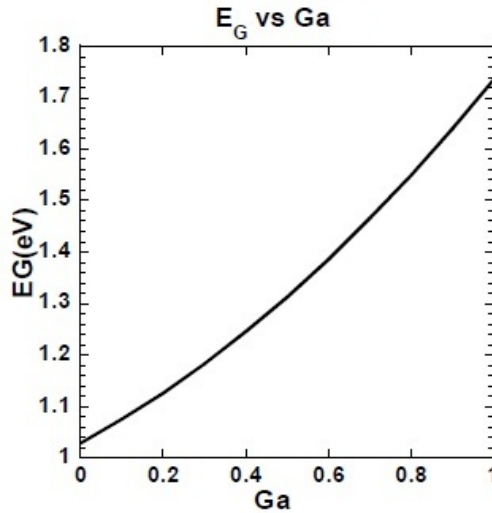


**Figure 3.2:**  $E_G$  vs Ga

Figure 3.2 shows the change in the band gap value with respect to addition of Ga to the alloy.

### 3.2 Electrical properties

Having a chalcopyrite structure,  $\text{Cu}(\text{In,Ga})\text{Se}_2$  films have various defect states which are controlled by compositional variation and thereby induced defects. Due to these intrinsic defects, the  $\text{Cu}(\text{In,Ga})\text{Se}_2$  structure is not fully understood and the study of electrical properties is difficult. But as an advantage, the band gap can be varied, which can be of use to find the optimum absorber material composition. Defect states within the gap vary significantly depending on the growth methods of the layer [14].

$\text{Cu}(\text{In,Ga})\text{Se}_2$  films can be made either p-type or n-type depending on the Cu/In ratio and the amount of Se [5,15]. Films deposited in a Se-rich environment will become p-type. For high quality photovoltaic devices, p-type  $\text{Cu}(\text{In,Ga})\text{Se}_2$  semiconductors are used [15].

The Cu/In ratio of the films also linearly affects charge carrier concentration as well as conductivity [5].

### 3.3 Optical properties

$\text{Cu}(\text{In,Ga})\text{Se}_2$  films have direct band gaps which means that light is absorbed more efficiently compared to Si solar cells which have indirect band gaps. Having a direct

band gap means that a photon can directly be emitted by an electron without loss of momentum and as a result, the material has a high absorption coefficient.

The band gap value of  $\text{CuIn}_x\text{Ga}_{1-x}\text{Se}_2$ , can be calculated according to the relation:

$$E_{g(x)} = 1.010 + 0.626 - bx(1-x) \quad (3.1)$$

where  $b$  is the bowing coefficient [4].

The formula for calculating the absorption coefficient of a direct bad gap material is:

$$\alpha = \frac{\ln[T/(1-R)^2]}{d} \quad (3.2)$$

where  $T$  is optical transmittance (%),  $R$  is reflectance (%) and  $d$  is the thickness of the film (cm) [4].

For  $\text{Cu}(\text{In,Ga})\text{Se}_2$  films, band gap varies from about 1.0 eV to 1.7 eV depending on the Ga concentration and the absorption coefficient is  $10^5 \text{ cm}^{-1}$ . The ability to control the band gap makes the production of graded-band gap devices possible, which helps improve the open circuit voltage and the short circuit current [16].

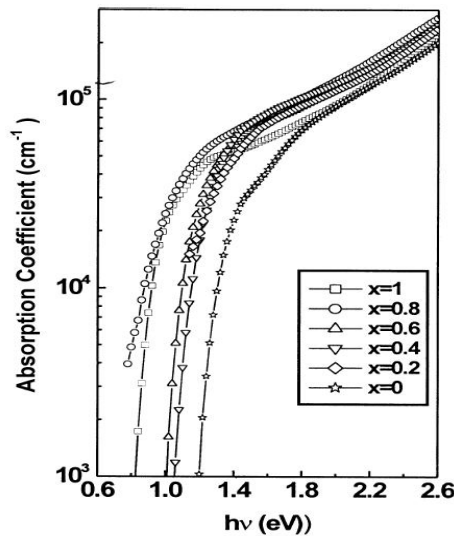


**Figure 3.3:** Absorption coefficient of  $\text{CuIn}_x\text{Ga}_{1-x}\text{Se}_2$  ( $x=1,0.8,0.6,0.4,0.2$  and  $0$ ) [17]

Figure 3.3 shows the variation in the optical absorption coefficient of  $\text{Cu}(\text{In,Ga})\text{Se}_2$  as a function of incident photon energy.



## **4. Cu(In,Ga)Se<sub>2</sub> THIN FILM DEPOSITION METHODS**

Besides trying to improve the conversion efficiencies of the solar cells, another important objective of the photovoltaic industry is to research deposition techniques to manufacture large area devices practically, at low cost.

Generally, the deposition method plays a significant role on the resulting film properties as well as on production cost. Cu(In,Ga)Se<sub>2</sub> thin films can be prepared from both gas and liquid phases by either physical or chemical deposition methods. There are a variety of techniques currently being researched. Common thin film deposition methods for CIS-based solar cells are co-evaporation from elemental sources, selenization of metallic precursor layers, evaporation from compound sources, chemical vapor deposition, closed-space vapor transport, and low-temperature liquid phase methods like electrodeposition, spray pyrolysis, and particle deposition techniques.

### **4.1 Co-evaporation**

Highest efficiency Cu(In,Ga)Se<sub>2</sub> solar cells have been obtained by co-evaporation method [18]. In this technique, compounds are vaporized and deposited on the substrate. This process takes place under high vacuum conditions and requires high substrate temperatures (>500°C). The most important aspect of this method is that the deposition rate can be controlled allowing the films to have homogeneous structure.

Although co-evaporation is the leading technology for depositing high quality films on small areas, but it exhibits problems for large area solar cell production. The need for controlling the evaporation flux of each element strictly results in waste of materials and high equipment costs. Also, the need for high temperature for film growth limits the selection of substrate materials. [2]

## **4.2 Sputtering**

In sputter deposition technique, material is ejected from a source, and then deposited onto the substrate. An important advantage of this method is that even materials with very high melting points can be easily deposited onto the substrate. Sputter deposited films have a composition close to that of the source material.

Compared to the co-evaporation technique, sputter deposition has higher throughput. More uniform films are composed and they have better adhesion on the substrate than evaporated films. Multilayer structure is produced in sputter deposition, and as a result better crystallinity is achieved.

Some disadvantages of the sputtering process are that the process is more difficult because the path the atoms will follow during process cannot be controlled and impurities can be obtained in the grown films. Additionally, the reaction rates of layers are different and separate phases can be formed if the reaction temperature is not high enough, or not held long enough. These conditions make the deposition process more complex and cause high equipment costs. [2]

An efficiency of 13.5% was obtained for small-area solar cells and above 7.5% efficiency was achieved for large-area modules [19].

## **4.3 Chemical vapor deposition**

Chemical vapor deposition is similar to co-evaporation and sputtering techniques in a sense that deposition takes place in gaseous phase. Its main difference from physical vapor deposition methods is that deposition takes place by chemical reactions. In a typical chemical vapor deposition process, the substrate is exposed to one or more vaporized compounds, which react on the substrate surface to produce the thin film.

Advantageously, high vacuum and high temperature conditions are uncalled for in chemical vapor deposition, and as a result, the production cost is reduced compared to physical vapor deposition techniques. Also, multi-source precursors can be used and large area films can be fabricated. But due to the difficulty of controlling the stoichiometry of the precursors and having a complex reaction mechanism, the resulting films are not very efficient and this technique is not commercially used to produce CIS-based solar cells. [2]



#### 4.4 Co-electrodeposition

Co-electrodeposition is the simplest electrochemical deposition method. It has numerous scientific, technological and economic advantages [7, 18, 20, 21, 22]:

- Suitable for growing uniform films over larger areas and for mass production
- Deposition of films can be done onto various types of substrates with different shapes and forms
- Deposition takes place at low temperatures
- Deposition rate is high and can be controlled easily
- It is a non-polluting method as the waste of chemicals is negligible
- The processing cost is low since electrodeposition does not require complex equipment and installations contrary to the high vacuum systems
- The price/efficiency ratio is very good

Efficiencies up to 15.4% have been obtained by the electrodeposition technique [7].

However, this technique still suffers from many problems associated with the control of chemical bath composition, applied deposition potentials, pH of the electrolyte, complexing agents, deposition time, and deposition temperature. It is crucial to control these parameters owing to their influence on the film properties and quality [Electrochemical growth of CuInSe<sub>2</sub> thin film on different].

Co-electrodeposition is an electrochemical method where Cu-In-Ga-Se compounds are present all together in a single chemical bath during deposition. This process, also called one-step electrodeposition, is the most investigated case due to the fact that it involves only one electrochemical process. In opposition to its simplicity, the electrochemical process becomes more complex, with the possibility of forming binary compounds in addition to the desired Cu(In,Ga)Se<sub>2</sub> phase in the film, such as Cu<sub>2</sub>Se, In<sub>2</sub>Se<sub>3</sub>. Obtained films are generally in amorphous state. To overcome this problem, thermal annealing post-treatments at high temperatures are applied to the deposited films. [5, 18, 23]



## 5. EXPERIMENTAL DETAILS

### 5.1 Experimental Setup

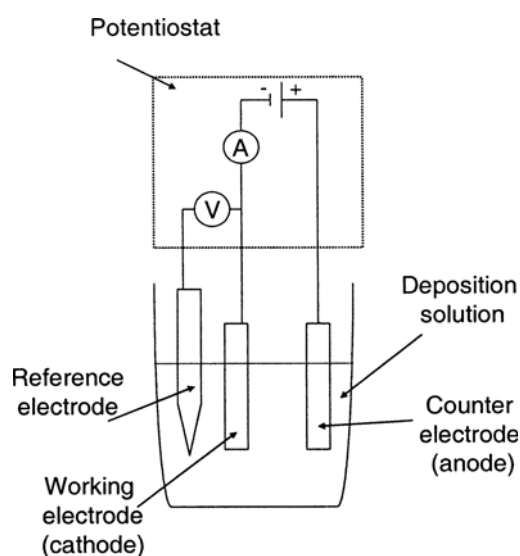


**Figure 5.1:** The three-electrode setup used in electrodeposition.

Figure 5.1 shows the schematic view of the three-electrode setup used in electrodeposition. The substrate is connected to the system as the working electrode which is connected to the power source as well as the counter electrode which ensures current flow through the circuit. The third electrode is the reference electrode which establishes the electrical potential against which other potentials may be measured. The potentiostat measures and controls the potential of the working electrode with respect to the reference electrode. [2]

About the electrochemical cell used in the experiments:

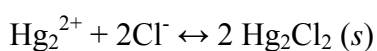
- Approximately 50 cm<sup>3</sup> volume
- Double layered glass wall
- Working electrode is placed in the center
- 2 entries for Na in and out flow

- 2 entries for reference and counter electrodes

The working electrodes used in the experiments were ITO-coated glass electrodes with a 1cmx2cm deposition area.

The counter electrode was Platinum gauze approximately with an area twice as large the working electrode.

The reference electrode was saturated calomel electrode (SCE). It has a redox potential of +0.2444V vs. Standard Hydrogen Electrode at 25°C. The electrode reaction takes place between the elemental mercury and the calomel (Hg<sub>2</sub>/Cl<sub>2</sub>), which are in contact with the saturated potassium chloride (KCl) solution. The cell notation is Hg/Hg<sub>2</sub>Cl<sub>2</sub>/KCl. The electrode reaction is given as follows:



## 5.2 Sample Preparation

Deposition bath used for the co-electrodeposition of CuInSe<sub>2</sub> films consisted of CuCl<sub>2</sub>, InCl<sub>3</sub>, and H<sub>2</sub>SeO<sub>3</sub>. Molar concentrations of the individual salts in the solution were: 4mM CuCl<sub>2</sub>, 2mM-4mM-8mM InCl<sub>3</sub> and 4mM-8mM H<sub>2</sub>SeO<sub>3</sub>. All deposition baths were prepared using a pH2.2 buffer solution, which is a mixture of KCl and HCl solutions. No complexing agents were used.

Before deposition, the ITO-coated glass substrates were kept in ultrasonic bath in acetone for approximately 5 minutes for cleaning. They were rinsed with deionized water and dried in flowing N<sub>2</sub> gas. Ohmic contact was provided by soldering copper wires on ITO. The contact point was wrapped around with Teflon and the substrate area to be immersed in the solution was measured to be approximately 1x2 cm<sup>2</sup>.

The films were co-electrodeposited by applying a constant voltage of -650mV for 15 minutes without stirring. The experiments were conducted at room temperature.

After deposition, the deposited films were rinsed with deionized water and dried in flowing N<sub>2</sub> gas. Some of the resulting films were annealed at 400°C with Argon gas for 30 minutes.

## 6. RESULTS AND CONCLUSION

### 6.1 Spectroscopy Results

ITO-coated glass was used as reference in spectroscopy measurements. The wavelength range was from 300nm to 1100nm. Band gap values were calculated according to equation (1.3).

Molar concentrations of the compounds in each sample solution were as follows:

Solution 1: (samples 1a-1b-1c): 4mM  $\text{CuCl}_2$ , 2mM  $\text{InCl}_3$ , and 8mM  $\text{H}_2\text{SeO}_3$ .

Solution 2: (samples 2a-2b-2c): 4mM  $\text{CuCl}_2$ , 4mM  $\text{InCl}_3$ , and 8mM  $\text{H}_2\text{SeO}_3$ .

Solution 3: (samples 3a-3b-3c): 4mM  $\text{CuCl}_2$ , 4mM  $\text{InCl}_3$ , and 4mM  $\text{H}_2\text{SeO}_3$ .

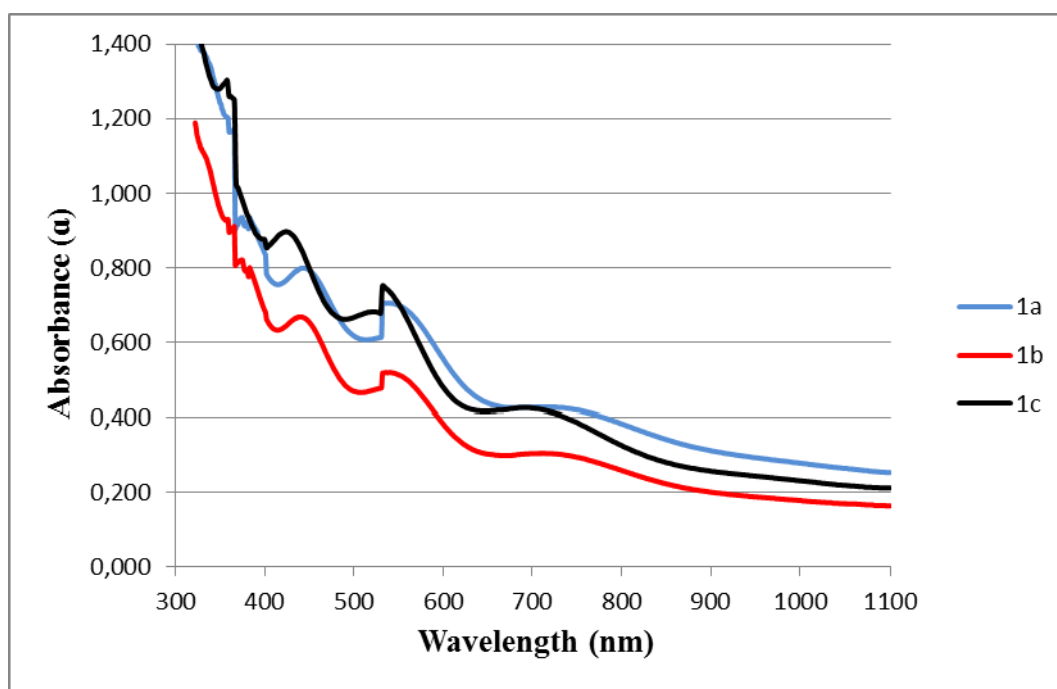


**Figure 6.1:** Optical absorbance ( $\alpha$ ) vs. wavelength (nm)

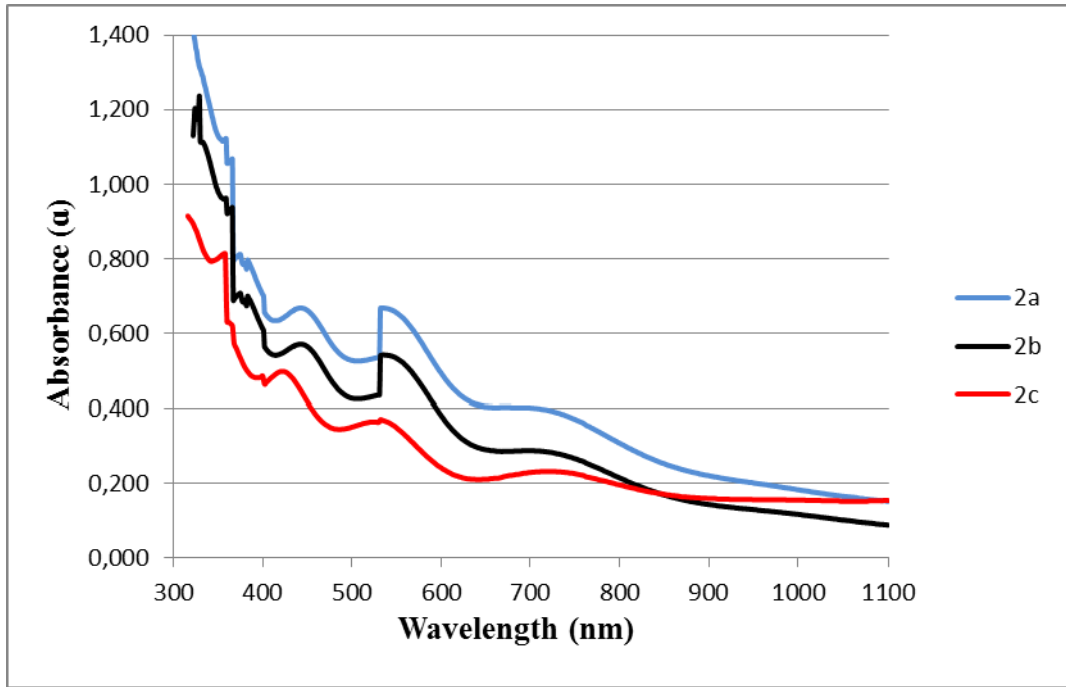


**Figure 6.2:** Optical absorbance ( $\alpha$ ) vs. wavelength (nm)

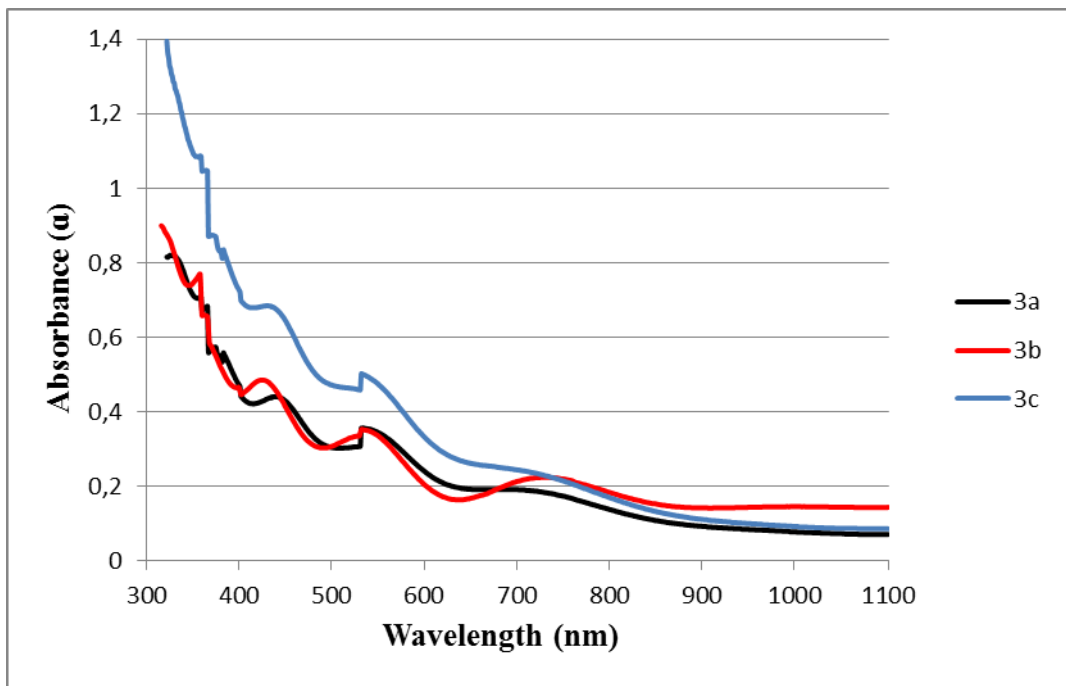


**Figure 6.3:** Optical absorbance ( $\alpha$ ) vs. wavelength (nm)

Figure 6.1, 6.2 and 6.3 shows the variation of the absorption of co-electrodeposited CIS thin films with wavelength.

From the graphs, it is seen that the samples electroplated in the solution with same molar concentrations show similar absorption values.

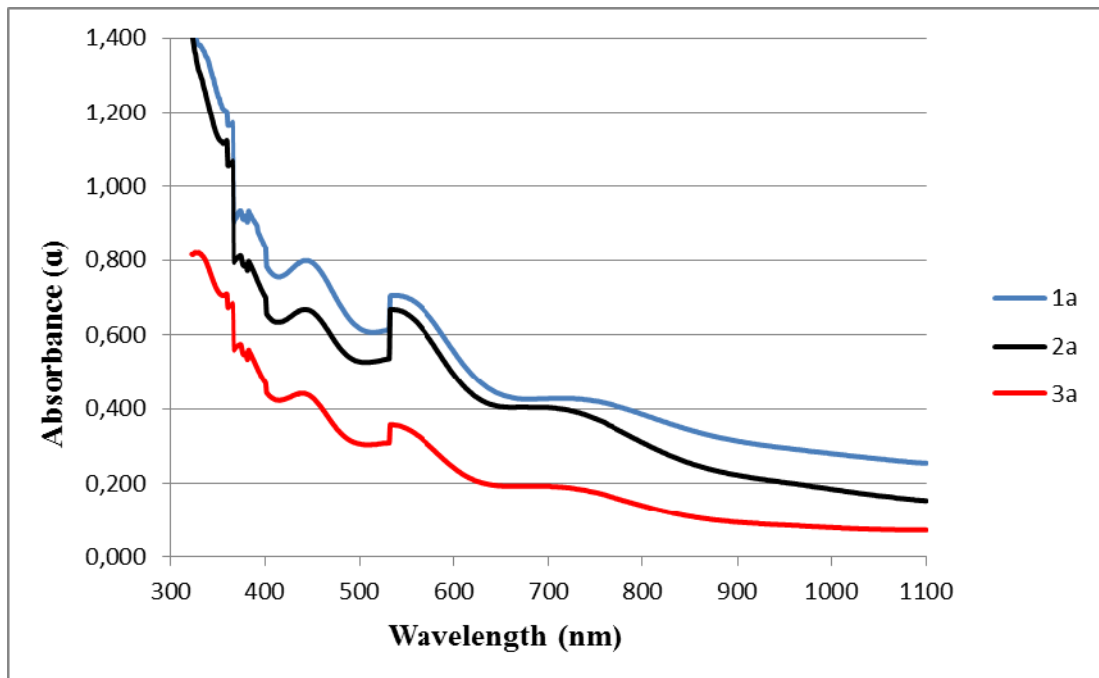


**Figure 6.4:** Optical absorbance ( $\alpha$ ) vs. wavelength (nm)

Figure 6.4 shows the variation of the absorption of co-electrodeposited CIS thin films with wavelength for different samples prepared in solutions with different molar concentrations.

As the Cu+In/Se ratio increases, the absorption value decreases. Highest absorption is obtained by sample 1a, prepared from the 4mM  $\text{CuCl}_2$ , 2mM  $\text{InCl}_3$ , and 8mM  $\text{H}_2\text{SeO}_3$  solution, but other samples also have similar values.

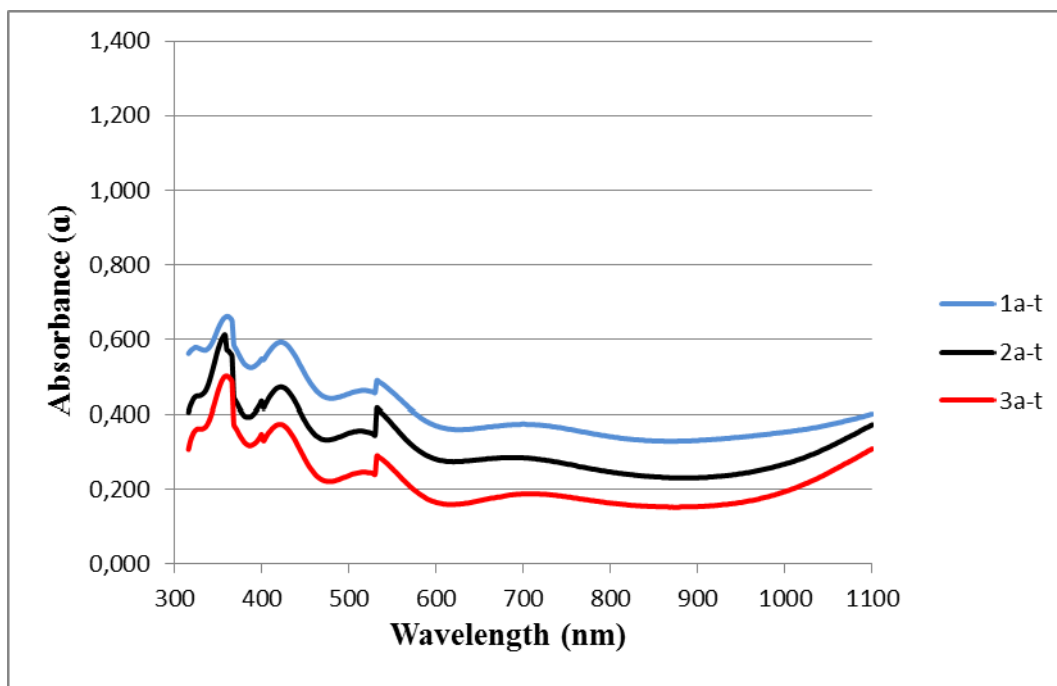


**Figure 6.5:** Optical absorbance ( $\alpha$ ) vs. wavelength (nm) after annealing

Figure 6.5 shows the variation of the absorption of annealed CIS thin films with wavelength.

Cu/In and Cu+In/Se ratios indicate the stoichiometry of the films. In figures 6.4 and 6.5 as the ratio of Cu/In decreases, and the Cu+In/Se ratio increases, it is seen that the higher energized photons are absorbed more. Also, figure 6.5 shows that there is additional absorption near the infrared region. This could be due to impurity states (undesired phases such as  $\text{Cu}_2\text{Se}$ ,  $\text{In}_2\text{Se}_3$ ) formed during the co-electrodeposition process.



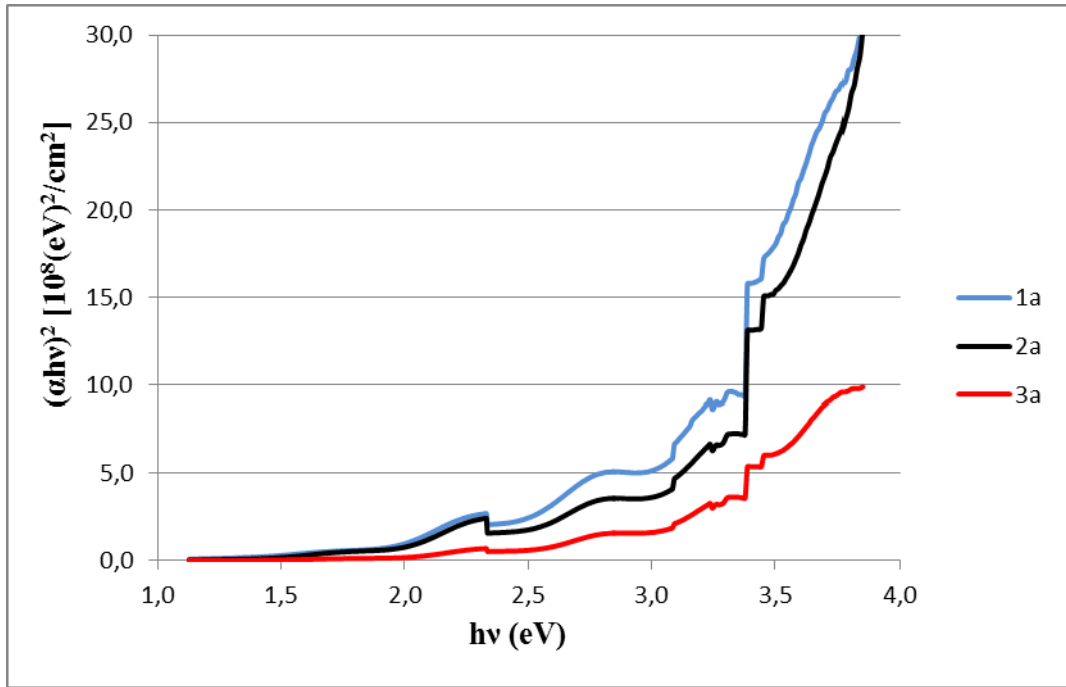


**Figure 6.6:**  $(\alpha hv)^2$  vs.  $hv$

Figure 6.6 shows the plot of  $(\alpha hv)^2$  vs.  $hv$ . The linear nature of the plot near the higher energy range indicates that the films have direct band gaps [20].

By extrapolating the linear fit of the plots to the energy axis at  $\alpha=0$ , the band gap values of the films are obtained. The band gap values of the films are

$E_{1a}=1.44\text{eV}$ ,  $E_{2a}=1.40\text{eV}$ ,  $E_{3a}=1.44\text{eV}$ , before annealing, and

$E_{1a-t}=1.21\text{eV}$ ,  $E_{2a-t}=1.10\text{eV}$ ,  $E_{3a-t}=1.08\text{eV}$ , after annealing.

The values show that as the Cu/In ratio increases and the Cu+In/Se ratio decreases, the band gap value increases. The values for annealed films are consistent with results given in reference articles.

## 6.2 XRD Results

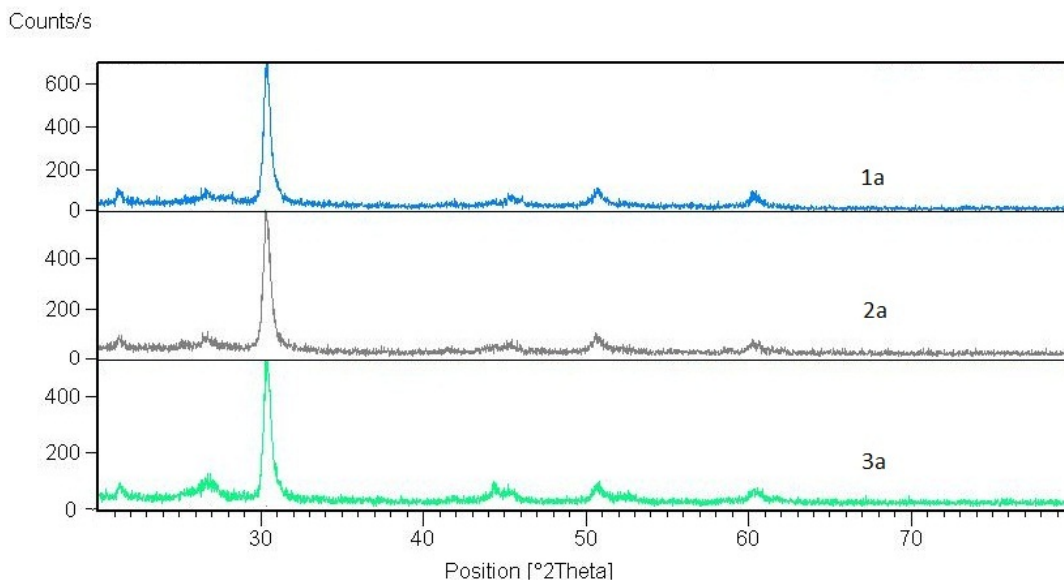


**Figure 6.7:** XRD patterns of CIS films

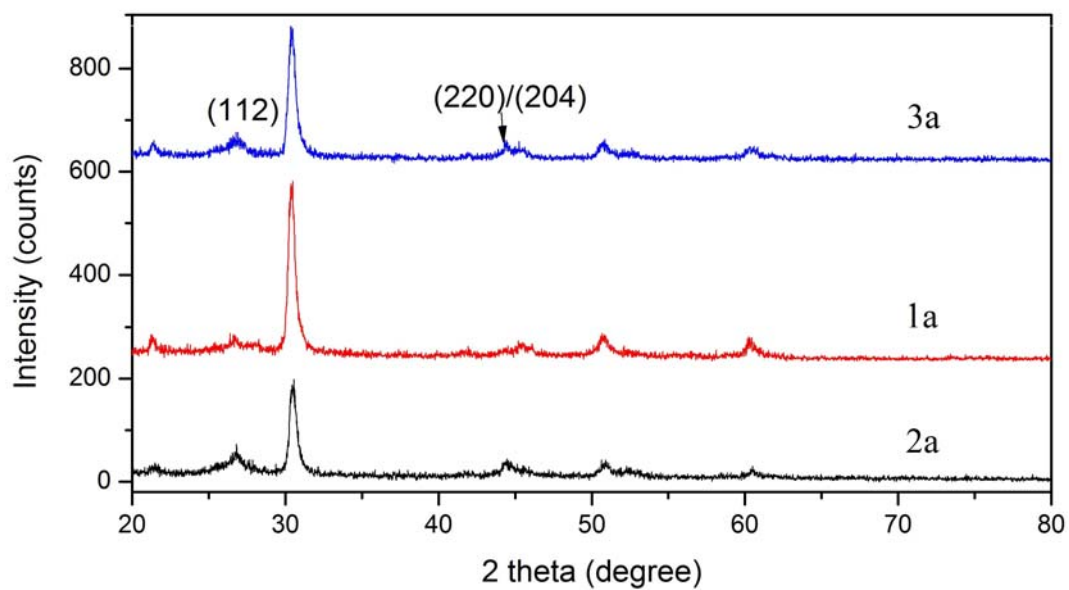


**Figure 6.8:** XRD patterns of CIS films

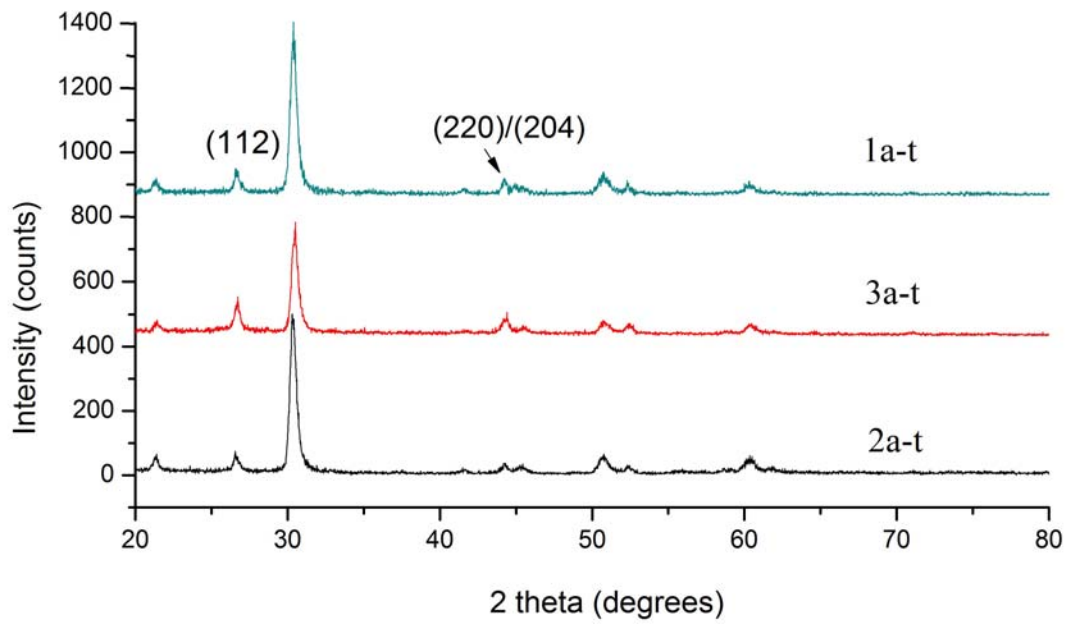


**Figure 6.9:** XRD patterns of CIS films annealed at 400<sup>0</sup>C for 30 min.

Figures 6.7 and 6.8 show the XRD results of the films before annealing. Peaks at 26.7°, 44.4°, 52.5° corresponding to the diffraction of (112), (220)/(204) and (116)/(312) planes confirm the CIS structure. The results indicate that films have chalcopyrite structure. The most intense peak seen on the graph is due to ITO.

Figure 6.9 shows the XRD results of the films after annealing. There is significant improvement of crystallinity between the two graphs (figures 6.8 and 6.9).

### 6.3 EDS Results

**Table 6.1:** EDS results in atomic percentage.

	O	Si	Cu	Se	In	Sn
ITO-glass	67.45	3.64			26.39	2.52
1-a	60.80	2.71	1.76	4.82	27.26	2.65
2-a	60.87	4.03	1.79	3.33	27.58	2.41
3-a	56.58	3.15	1.75	5.64	29.98	2.90

**Table 6.2:** EDS results in atomic percentage for annealed samples.

	O	Si	Cu	Se	In	Sn
1a-t	38.71	3.50	3.72	18.55	33.36	2.15
2a-t	45.20	2.79	3.28	12.74	33.94	2.06
3a-t	50.58	3.96	3.26	8.64	31.05	2.51

**Table 6.3:** Cu/In and (Cu+In)/Se ratios of films.

	<b>Cu/In</b>	<b>(Cu+In)/Se</b>
1-a	0.065	<b>6.021</b>
2-a	0.065	<b>8.820</b>
3-a	0.058	<b>5.626</b>
1a-t	0.112	<b>1.999</b>
2a-t	0.097	<b>2.922</b>
3a-t	<b>0.105</b>	<b>3.971</b>

The EDS results in tables 6.1, 6.2 and 6.3 show the chemical compositions and Cu/In and (Cu+In)/Se of the films before and after annealing treatments.

It can be concluded that the annealing treatments help improve the stoichiometry of the films. Also, it is seen that the 4mM CuCl<sub>2</sub>, 2mM InCl<sub>3</sub>, and 8mM H<sub>2</sub>SeO<sub>3</sub> solution give better atomic percentage results.

## 6.4 SEM Results

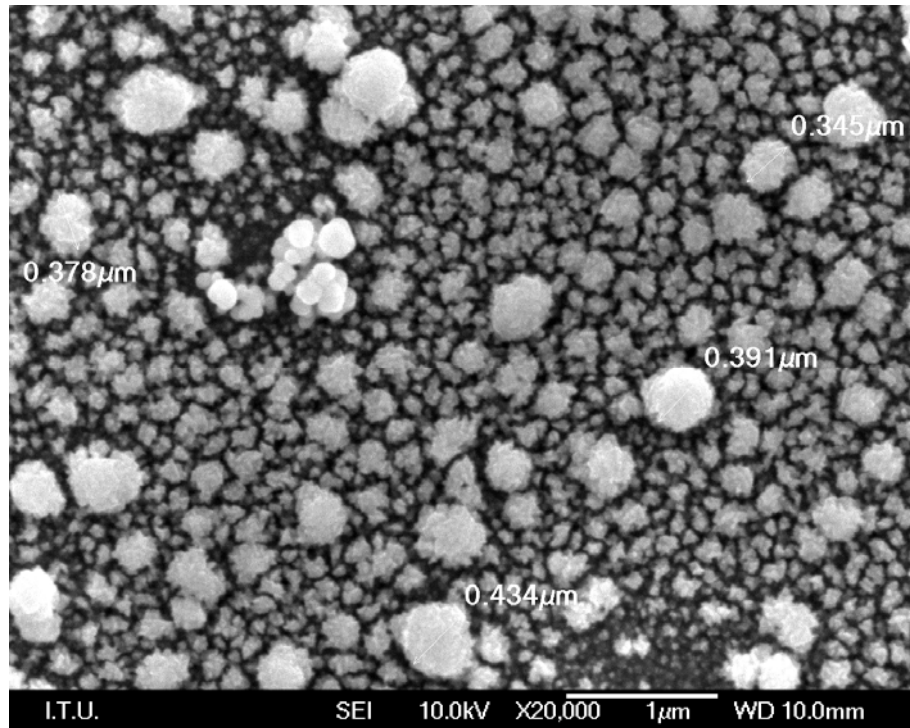


Figure 6.10: SEM image of sample 1a

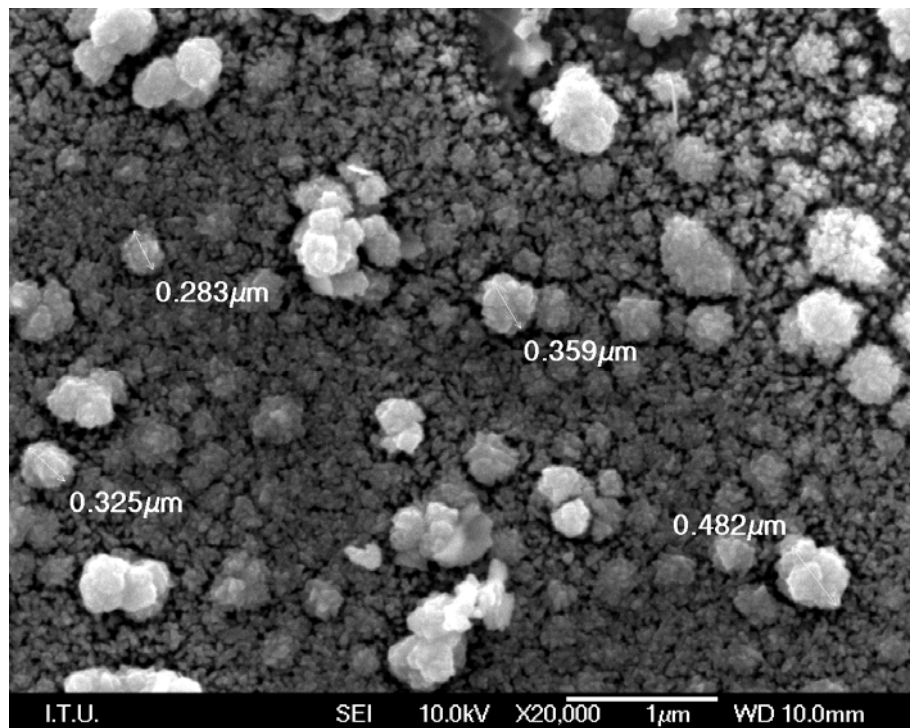
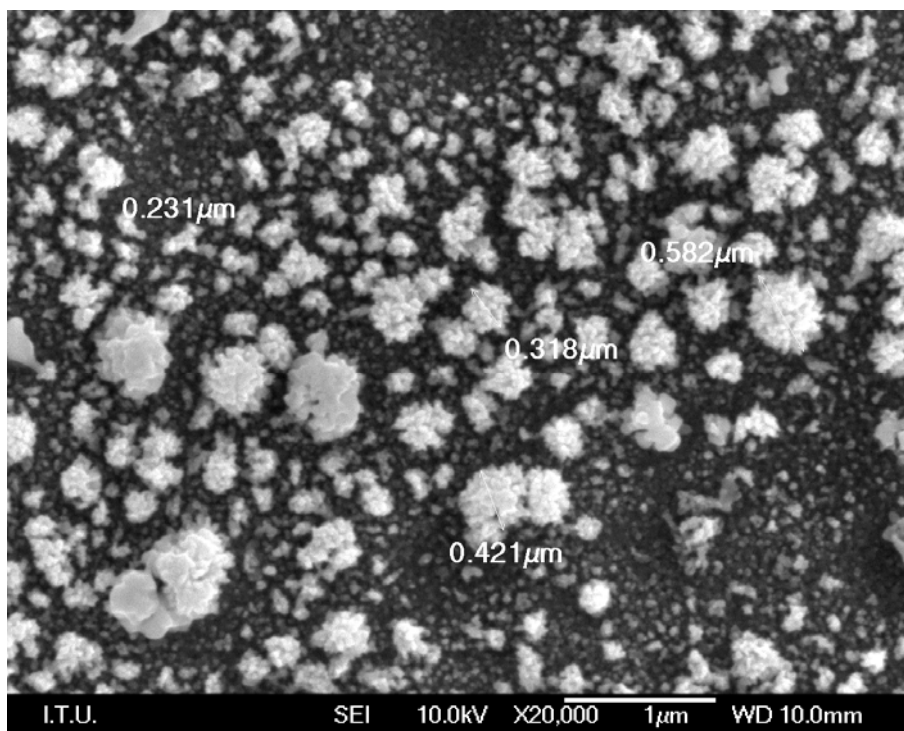


Figure 6.11: SEM image of sample 2a



**Figure 6.12:** SEM image of sample 3a

Figures 6.10, 6.11 and 6.12 show the SEM images at magnification (x 20,000) for samples 1a, 2a and 3a respectively.

The overall compositions of the three substrates are similar to each other. The grain sizes are small and vary from ~200nm to ~600nm. The samples are not smooth or homogeneous, but the morphology is more compact and grain size is bigger in sample 1a, as the Cu/In ratio increases.

## 6.5 Conclusion

In this study, CIS electrodeposited ITO glass substrates were analyzed. The effects and importance of different molar concentrations of salts in the electrodeposition bath and annealing for improving electrochemically prepared CIS solar cells were examined.

The spectroscopy, X-Ray diffraction, energy dispersive spectroscopy and scanning electron microscopy results show that higher absorption, better band-gap value, bigger grain size, more compact structure and better stoichiometry is obtained by the samples 1a, 1b and 1c; so it can be concluded that the molar concentration of salts in solution 1, which include 4mM  $\text{CuCl}_2$ , 2mM  $\text{InCl}_3$ , and 8mM  $\text{H}_2\text{SeO}_3$ , give the best results.

The results also point out that annealing is an important step for preparation of CIS films. The annealed samples have better band-gap values and better crystallinity when compared to the results of the unannealed samples.

This study shows that electrodeposition is a powerful way to produce CIS thin films. This technique is easy to conduct experiments in the university laboratory. It is a fast process to get quick results, and also cheap and safe.

However, wider variety of structures with different parameters should be investigated to get better composition and morphology results. Temperature can be controlled to get more certain results for comparison. And complexing agents can be used to shift the deposition potentials of the salts.



## 7. REFERENCES

- [1] **N.S. Lewis**, 2005, Basic Research Needs for Solar Energy Utilization, Report on the Basic Energy Sciences Workshop on Solar Energy Utilization, U.S. Department of Energy Office of Basic Energy Sciences.
- [2] **Marianna Kemell, Mikko Ritala, and Markku Leskela**, 2005, Thin Film Deposition Methods for CuInSe<sub>2</sub> Solar Cells, *Critical Reviews in Solid State and Materials Sciences*, 30:1–31.
- [3] **Armin G. Aberle**, 2009, *Thin Solid Films*, 517, 4706–4710.
- [4] **F Kang, J P Ao, G Z Sun, Q He and Y Sun**, 2009, *Semicond. Sci. Technol.* 24, 075015.
- [5] **Xia Donglin, Xu Man, Li Jianzhuang, Zhao Xiujian**, 2006, *J Mater Sci* 41, 1875–1878.
- [6] **T. P. Gujar, a V. R. Shinde, Jong-Won Park, Hyun Kyung Lee, Kwang-Deog Jung, and Oh-Shim Joo**, 2009, *Journal of The Electrochemical Society*, 156 (1) E8-E12.
- [7] **R.N. Bhattacharya, J.F. Hiltner, W. Batchelor, M.A. Contreras, R.N. Noufi, J.R. Sites**, 2000, *Thin Solid Films*, 361-362, 396-399.
- [8] **D.M. Chapin, C.S. Fuller, G.L. Pearson**, 1954, *J. Appl. Phys.* 25, 676-677.
- [9] **Martin A. Green**, 2009, *Prog. Photovolt: Res. Appl.* 17:183-189.
- [10] **S. Guha**, 2005, *Proc. 31st IEEE PVSC*, Lake Buena Vista, FL, 12-16.
- [11] **A. J. Breeze**, 2008, Next Generation Thin-Film Solar Cells, *Reliability Physics Symposium*, 168-171.
- [12] **B. Dimmler, M. Powalla, R. Schaeffler**, 2005, *Proc. 31st IEEE PVSC*, Lake Buena Vista, FL, 189-194.
- [13] **Kasturi L. Chopra, Suhit Ranjan Das**, 1983, *Thin Film Solar Cells*, Plenum Press.
- [14] **L. L. Kerr, S. S. Li, S. W. Johnston, T. J. Anderson, O. D. Crisalle, W. K. Kim, J. Abushama, R. N. Noufi**, 2004, *Solid-State Electronics* 48, 1579-1586.
- [15] **A.M. Hermann, C. Gonzalez, P.A. Ramakrishnan, D. Balzar, N. Popa, P. Rice, C.H. Marshall, J.N. Hilfiker, T. Tiwald, P.J. Sebastian, M.E. Calixto, R.N. Bhattacharya**, 2001, *Solar Energy Materials & Solar Cells* 70, 345–361
- [16] **R. Friedfeld, R.P. Raffaele, J.G. Mantovani**, 1999, *Solar Energy Materials & Solar Cells* 58, 375-385.

- [17] **C.A.D. Rincón, E. Hernández, M.I. Alonso, M. Garriga, S.M. Wasim, C. Rincón and M. León**, 2001, *Materials Chemistry and Physics*, 70, 300.
- [18] **D. Lincot, J.F. Guillemoles, S. Taunier, D. Guimard, J. Six-Kurdi, A. Chaumont, O. Roussel, O. Ramdani, C. Hubert, J.P. Fauvarque, N. Bodereau, L. Parissi, P. Panheleux, P. Fanouillere, N. Naghavi, P.P. Grand, M. Benfarah, P. Mogensen, O. Kerrec**, 2004, *Solar Energy* 77, 725–737.
- [19] **N.G. Dhere**, 2007, *Solar Energy Materials & Solar Cells*, 91, 1376.
- [20] **Soon Hyung Kang, Yu-Kyung Kim, Don-Soo Choi, Yung-Eun Sung**, 2006, *Electrochimica Acta* 51, 4433–4438.
- [21] **A.M. Fernandez, M.E. Calixto, P.J. Sebastian, S.A. Gamboa, A.M. Hermann, R.N. Noufi**, 1998, *Solar Energy Materials and Solar Cells* 52 423-431.
- [22] **M. Burada, V. Soare, D. MitricĂ, C. P. Lungu, V. Ghenescu, L. Ion**, 2009, *METALURGIA INTERNATIONAL* vol. XIV special issue no. 3, 193-196.
- [23] **P.J. Sebastian, M.E. Calixto, R.N. Bhattacharya, Rommel Noufi**, 1999, *Solar Energy Materials & Solar Cells* 59, 125-135
- [24] **S. Carroll, M.M. Marei, T.J. Roussel, R.S. Keynton, R.P. Baldwin**, 2011, *Sensors and Actuators B: Chemical*, 160, 318.

## **CURRICULUM VITAE**

**Name:** Gizem Őanlı

**Date and Place of Birth:** 1985, İstanbul

**Address:** Kadıköy, İstanbul

**Education:** Kadıköy Anadolu Lisesi, İstanbul, 2004

BS in Physics, Middle East Technical University (METU), Ankara,2008

**Publications:** Őanlı, G., Kadirgan, F. 2012: Investigation of Electrochemically Deposited CIS(Cu-In-Se) Solar Cells, *NANO TR8*, June 2012, Ankara, Turkey